Driven Granular Gases

Stefan Luding[1,2], Raffaele Cafiero[3], and Hans J. Herrmann[2]

[1] Particle Technology, DelftChemTech, TU Delft,
Julianalaan 136, 2628 BL Delft, The Netherlands
e-mail: s.luding@tnw.tudelft.nl

[2] Institute for Computer Applications 1, University of Stuttgart,
Pfaffenwaldring 27, 70569 Stuttgart, Germany
e-mail: lui@ica1.uni-stuttgart.de

[3] P.M.M.H., École Supérieure de Physique et de Chimie Industrielles (ESPCI)
10, rue Vauquelin, 75251 Paris CEDEX 05, France

Summary. In this paper, a two-dimensional granular gas of inelastic, rough spheres subject to driving is examined. Either the translational degrees of freedom are agitated proportional to a power $|v(\vec{x})|^\delta$ of the local particle velocity $v(\vec{x})$, or the rotational degrees are agitated randomly with respect to the angular velocity $\omega(\vec{x})$.

The steady state properties of the model, with respect to energy, partition of energy, and velocity distributions, are examined for different values of δ, and compared with the homogeneous driving case $\delta = 0$. A driving linearly proportional to $v(\vec{x})$ seems to reproduce some experimental observations which could not be reproduced by a homogeneous driving. Furthermore, we obtain that the system can be homogenized even for strong dissipation, if a driving inversely proportional to the velocity is used ($\delta < 0$). In the case of rotational driving, the system is well randomized and clusters are hindered. Even though rotational driving may be difficult to realize experimentally, this is an opportunity to avoid or delay the often unwanted effect of clustering.

PACS: 45.70, 47.50+d, 51.10.+y, 47.11.+j

1 Introduction

Granular materials belong to the fascinating world of non-linear, dissipative, non-equilibrium systems [1–3]. Hard spheres, as a special case, are used also as basic model for gases, liquids, and e.g. glasses [4]. Adding dissipation and rotation to hard spheres, one has the simplest yet realistic model granulate. Granular media are (more complicated) collections of macroscopic particles with rough surfaces and dissipative, frictional interactions, but also involve eigen-modes of vibration and possibly plastic deformation or fracture. Disregarding the latter two, one has Molecular dynamics (MD) simulations as an established tool to complement advanced theoretical approaches and difficult experimental studies.

Granular gases are the more dynamic limit of granular media as opposed to static systems. One of the outstanding effects in granular gases is the so called clustering, a self-stabilized density instability due to dissipation [5–7], where large, dense collections of particles co-exist with almost empty areas. Clustering occurs in initially homogeneous systems [5–9, 50] and should not be confused with the so-called "inelastic collapse" [5, 10], the divergence of the collision rate, which is inherent to the frequently used hard (rigid) sphere model [5, 6, 11, 12]. Freely cooling systems – mainly examined numerically and theoretically – are almost impossible to realize experimentally. Only in the last years, laboratory experiments were performed, where clustering could be examined in driven systems [13–19], where also kinetic theory approaches [20–28, 51] complemented by numerical simulations have proven to be successful [11, 24, 29–34].

The driving of a granular material can be realized by moving walls [2, 35] which lead to local heating and possibly shock-waves [49], or the system can alternatively be driven by a global homogeneous, random energy source in different variations [11, 24, 28, 32, 36–39]. The latter type of energy input does not exactly resemble the experimental situation, where a two-dimensional (2D) horizontal layer of spheres is agitated by vertical vibrations of the bottom surface and the horizontal degrees of freedom are indirectly agitated due to the different vertical jump heights of the colliding particles [14, 18, 19, 34]. Translational energy input (due to vibrations) was also applied for other boundary conditions and a variety of interesting experimental results were obtained just recently [13–16, 18, 19, 40].

Generic seems to be that one can obtain a gas and a liquid state, together with dense, solid-like clusters which form due to dissipation. Thus, the choice of the driving term to put into a theory for dissipative systems is an open problem and we expect that it depends on the nature of the driving (vibrating wall, airflow, Brownian noise, etc.). In this paper we present a more detailed and complete study as in [11, 12] and also combine both approaches in the framework of a mean field theory for the evolution to the steady state.

In [11], in order to find possible candidates for a realistic energy input, the inelastic hard sphere (IHS) model with an inhomogeneous, *multiplicative driving* was examined. The driving is proportional to the local velocity $|v(\vec{x})|^\delta$, with a given power δ which can take both positive and negative values. The classical homogeneous driving with $\delta = 0$ is contained in our approach as a special case. A positive power leads to weak energy input for slow particles, e.g. those moving collectively inside a cluster [14, 18, 34]. We present a series of results from numerical simulations performed for different sizes N of the system, different values of r and different exponents δ of the driving. Then we compare our results with an analytical MF approach.

A driving linearly proportional to $v(\vec{x})$ ($\delta = 1$) seems to reproduce some experimental observations which could not be reproduced by a homogeneous driving, like an anticipated onset of clustering with respect to the case of homogeneous driving, stable clustering in equilibrium with a low density (gas)

phase, anomalous velocity distribution in the clustering regime with exponents different from the value 3/2 obtained analytically and numerically for the case with homogeneous driving [41]. Furthermore, we obtain that the system can be homogenized even for strong dissipation, if a driving inversely proportional to the velocity is used ($\delta < 0$).

Depending on the experimental setup, energy can be given to the translational degrees of freedom or, alternatively, to the rotational ones, or to both. Since the first case catched most of the attention, we change the focus and feed also rotational energy instead of translational. Driving of the rotational degrees of freedom is scarcely realized so far [M. Markus, private communication, A. Kudrolli, private communication, D. Wolf, private communication], and requires either electro- or magneto-dynamic forces in order to couple the rotational degrees of freedom. Such a situation could correspond, for example, to a gas of rough magnetic particles subject to a rapidly varying, homogeneous, magnetic field. Besides a possible experimental application, we believe that this study is interesting in itself. We examine the case of isolated rotational driving, since the correct modeling of the driving mechanism is of great importance for a theory of granular gases to describe realistic experimental situations. In the future, translational and rotational driving can also be combined, however, we focus only on the isolated cases here because this allows at least partially for analytical solutions.

The paper is organized as follows. Section II introduces and describes the model, and in section III we the mean field (MF) equations for the model with multiplicative translational driving and homogeneous rotational driving are provided. In section IV we present numerical simulations for translationally driven smooth particles, and compare numerical results with analytical predictions. Section V is devoted to the comparison of simulations of rotationally driven particles with theory. A study of the velocity distributions, and in particular of its high energy tail follows in section VI, and in section VII we draw the conclusions of our study and outline future research directions.

As a remark to our nomenclature. When we write steady state in the following, this has to be understood as non-equilibrium steady state (NESS) [32]. Furthermore, the word equilibrium means a state of the system, where energy-input and dissipation cancel each other so that energy-loss and energy-input rates are in "equilibrium"; we do not have an equilibrium in the classical sense here.

2 The model

In this section the numerical model is introduced and a few typical examples of the simulation are presented in Fig. 1.

A system of N three-dimensional spheres with radius a and mass m is considered, interacting via a hard-core potential and confined to a 2D plane of linear extension L, with periodic boundary conditions. The degrees of freedom

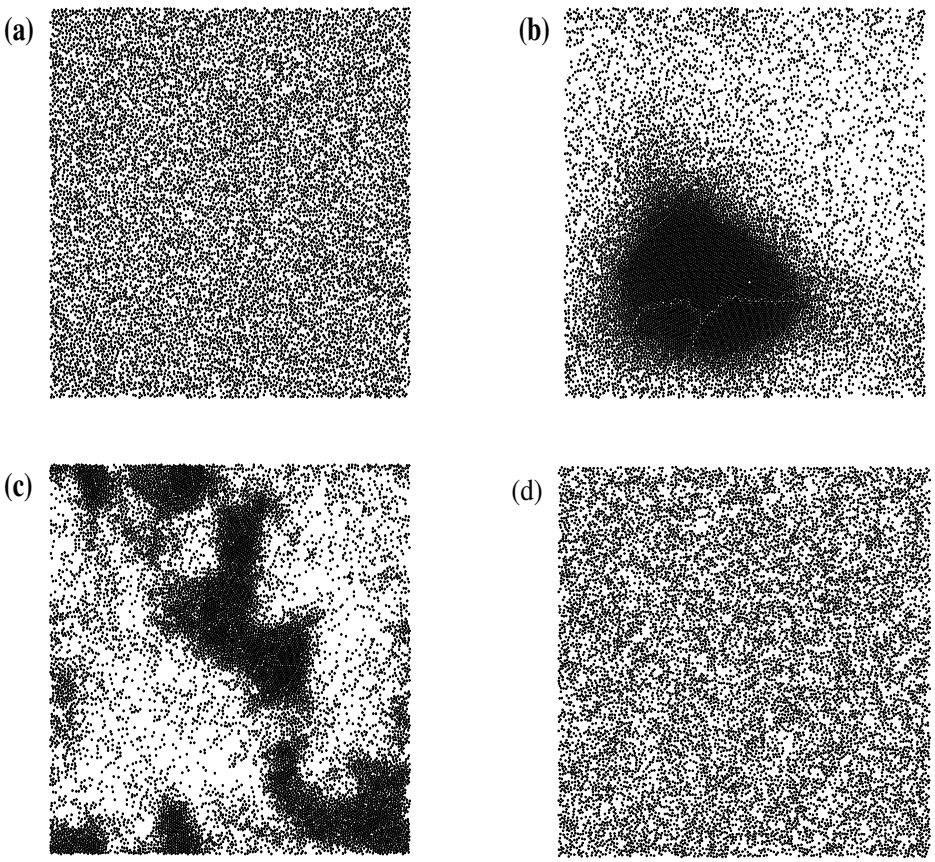

Fig. 1. Snapshots of the particle distribution in the steady state for a system of $N = 11025$ smooth ($r_t = -1$) particles, $\delta = 1$, $\nu = 0.34$, and $H_{\rm dr} = 1.0\,{\rm s}^{-1}$, with $r = 0.999$ (a), $r = 0.97$ (b), and $r = 0.6$ (c). In panel (d), a snapshot of the particle distribution in the steady state for a rotationally driven system of $N = 11025$ particles, $\nu = 0.34$, $r_t = 1$, and $r = 0.1$ is shown for $J = 1.0\,{\rm s}^{-1}$.

are the positions $\vec{r}_i(t)$, the translational velocities $\vec{v}_i(t)$, and the rotational velocities $\vec{\omega}_i(t)$ for each sphere numbered by $i = 1, \ldots, N$.

2.1 Dissipation on collisions

The dissipation at a collision (in normal direction) is quantified by a constant normal restitution r. From the momentum conservation law and the rule $\vec{v}\,'^{(n)}_{\rm c} = -r\vec{v}^{(n)}_{\rm c}$, where the prime denotes the value after the collision, one can derive the change of linear momentum $-(m/2)(1+r)\vec{v}^{(n)}_{\rm c}$ of particle i, which

collides with particle j. The normal relative velocity is $\vec{v}_{\mathrm{c}}^{(n)} = [(\vec{v}_i - \vec{v}_j) \cdot \vec{n}]\vec{n}$, and the unit vector in normal direction is $\vec{n} = (\vec{r}_i - \vec{r}_j)/|\vec{r}_i - \vec{r}_j|$. The dissipation in tangential direction is quantified by the (constant) tangential restitution r_t, such that $\vec{v}\,'^{(t)}_{\mathrm{c}} = -r_t \vec{v}_{\mathrm{c}}^{(t)}$.

The magnitude of dissipation is proportional to $1 - r^2$ (normal) and $1 - r_t^2$ (tangential), while the strength of the coupling between rotational and translational motion is connected to $1 + r_t$, where the (constant) normal restitution r can vary between 1 (elastic) and 0 (inelastic) and the tangential restitution r_t varies between -1 (smooth) and $+1$ (rough), corresponding to zero and maximum coupling, respectively [6, 9, 21, 42]. The details of more realistic contact models are discussed in other chapters in this book [47, 48].

2.2 Translational, multiplicative driving

The system is agitated each time interval $\Delta t = f_{\mathrm{dr}}^{-1}$, with a driving rate f_{dr} (in the experiment this is according to the frequency of the vibrating bottom). For homogeneous driving, it is costumary to assume $f_{\mathrm{dr}} \gg t_n^{-1}$, where t_n^{-1} is the collision frequency of the granular gas. This, however, does not correspond to the experiments, were f_{dr} can be rather small [14, 18, 19]. In our simulations we will use driving frequencies around $100\,\mathrm{s}^{-1}$ comparable to those used experimentally [14, 18]. We did numerical checks with strongly different values of f_{dr} and found a similar behavior of the system even for driving frequencies lower than, but of the same order as t_n^{-1}, provided that a stationary state is reached.

Every time interval Δt, the velocity of particle i is changed:

$$\begin{aligned} v_i'^x(t) &= v_i^x(t) + r_i^x |\vec{v}_i(t)|^\delta v_r^{1-\delta} \\ v_i'^y(t) &= v_i^y(t) + r_i^y |\vec{v}_i(t)|^\delta v_r^{1-\delta} \ , \end{aligned} \tag{1}$$

where the driving occurs at time t and the prime on the left hand side indicates the value after the driving event. v_r is a reference velocity (in this study we use $v_r = 1\,\mathrm{m\,s}^{-1}$) which allows to define the dimensionless translational particle temperature $T = E/(NT_r)$, with $E = (m/2)\sum_{i=1}^N \boldsymbol{v}_i^2$ and the reference temperature $T_r = mv_r^2$. The variance of the uncorrelated Gaussian random numbers r_i^x and r_i^y (with zero mean) can now be interpreted as a dimensionless driving temperature T_{dr}.

The power δ is a parameter that takes into account the type of driving. In the special case of $\delta = 0$, one has random driving, as typically used in the literature. The random numbers are dimensionless and v_r provides the dimension and scale of the driving velocity. For $\delta > 0$, particles with large velocities obtain overproportional energy input, whereas in the case $\delta < 0$ slow particles obtain stronger energy input as compared to fast particles. The former case resembles the experimental situation in so far that particles with slow relative velocities presumably move in phase and thus obtain less energy input than particles that move out of phase.

The stochastic driving rule in Eq. (1) leads thus to an average rate of change of temperature

$$\Delta T/\Delta t = H_{\rm dr} T^{\delta} \quad \text{with} \quad H_{\rm dr} = f_{\rm dr} T_{\rm dr} \ . \tag{2}$$

In the next section we introduce this driving rate in the MF equation for the evolution of T [6], but first the case of rotational driving is discussed.

2.3 Rotational driving

In the case of a rotational driving event, with frequency $f_{\rm dr}$, see above, the translational velocity remains unchanged, but the angular velocity ω_i of particle i is modified at each time of agitation t so that

$$\omega_i'(t) = \omega_i(t) + r_i^{\omega}\, \omega_0, \tag{3}$$

where the prime on the left hand side indicates the value after the driving event. Due to the two-dimensionality of the system, we apply the driving force only to the z-direction, so that the scalar ω is to be understood as the z-component of $\vec{\omega}$.

The reference angular velocity, ω_0, allows to define the dimensionless translational and rotational particle temperatures

$$T_{\rm tr} = E_{\rm tr}/(NT_0) \ , \tag{4}$$

and

$$T_{\rm rot} = 2E_{\rm rot}/(NT_0) \ , \tag{5}$$

with the translational energy $E_{\rm tr} = (m/2)\sum_{i=1}^{N} \vec{v}_i^{\,2}$, the rotational energy $E_{\rm rot} = (qma^2/2)\sum_{i=1}^{N} \vec{\omega}_i^{\,2}$ (with the moment of inertia prefactor $q = 2/5$ for $3D$ spheres), and the reference temperature $T_0 = mv_0^2$, with $v_0 = a\omega_0$. The variance of the uncorrelated Gaussian random numbers r_i^{ω} (with zero mean) can now be interpreted as a dimensionless driving temperature $T_{\rm dr}^{\omega}$ [12]. The stochastic driving leads thus to an average rate of change of temperature

$$\Delta T_{\rm rot}/\Delta t = J_{\rm dr} \ , \quad \text{with} \quad J_{\rm dr} = f_{\rm dr} T_{\rm dr}^{\omega} \ . \tag{6}$$

In the case of driving of the translational degrees of freedom, the reference temperature T_r will be used, whereas in the case of rotational driving, the reference T_0 will be used for scaling.

3 Mean field evolution equations

The starting point for our mean-field analysis is the theory of Huthmann and Zippelius [9], for a freely cooling gas of infinitely rough particles, which was recently complemented by event driven (ED) simulations in 2D and 3D [6]

and by studies of driven systems as well [11, 12]. The main outcome of this approach is a set of coupled evolution equations for the translational and rotational MF temperatures $T_{\rm tr}$ and $T_{\rm rot}$ [6, 9], which can be extended to describe arbitrary energy input (driving) [11, 12]. The equations were derived assuming uncorrelated collisions and a Maxwellian velocity distribution, together with the contact model assumptions as described above.

In the present study, given the random driving temperatures $T_{\rm dr}$ or $T_{\rm dr}^{\omega}$ and an energy input rate $f_{\rm dr}$, as defined above, one just has to add the positive rate of change of translational energy $H_{\rm dr}$ and rotational energy $J_{\rm dr}$ to the system of equations:

$$\frac{d}{dt}T_{\rm tr}(t) = G\left[-AT_{\rm tr}^{3/2} + BT_{\rm tr}^{1/2}T_{\rm rot}\right] + H_{\rm dr}T^{\delta} \ , \tag{7}$$

$$\frac{d}{dt}T_{\rm rot}(t) = 2G\left[BT_{\rm tr}^{3/2} - CT_{\rm tr}^{1/2}T_{\rm rot}\right] + J_{\rm dr} \ , \tag{8}$$

with

$$G = \frac{8\nu g(\nu)}{a\sqrt{\pi m}} \ , \tag{9}$$

and the pair correlation function at contact $g(\nu) = (1 - 7\nu/16)/(1 - \nu)^2$ in the approximation proposed by Henderson and Verlet&Levesque [43, 44], dependent only on the volume fraction of the granular gas $\nu = \pi a^2 N/V$. The constant coefficients in Eqs. (7) and (8) are

$$A = (1 - r^2)/4 + \eta(1 - \eta)/2 \ ,$$

$$B = \eta^2/(2q) \ , \text{ and} \tag{10}$$

$$C = \eta\,(1 - \eta/q)\,/(2q) \ , \tag{11}$$

with the abbreviation $\eta = \eta(r_t) = q(1 + r_t)/(2q + 2)$, as derived and used in Refs. [6, 9].

Typical steady-state configurations for translational driving for different r values are shown in Fig. 1(a-c), and a snapshot for rotational driving is shown in Fig. 1(d).

3.1 Smooth particles – no rotation

The time evolution equation of $T = T_{\rm tr}$ was derived for the case of a freely cooling granular gas by means of a pseudo-Liouville operator formalism [6, 9]. We adopt the nomenclature and account for the driving by adding Eq. (2) to the mean field (MF) equation for the translational degree of freedom

$$\frac{d}{dt}T(t) = -G_r A T^{3/2} + H_{\rm dr}T^{\delta} \ . \tag{12}$$

For our case of a homogeneous monolayer of smooth spheres, one has $G_r = 8an\sqrt{\pi T_r/m}g(\nu)$, and $A = (1-r^2)/4$, with the number density $n = N/V$, the

pair correlation function at contact $g(\nu)$, and the area fraction ν covered by particles [6, 9, 11]. For $\delta = 0$ the driving is homogeneous and independent of the local granular temperature (or velocity), and one can identify our energy input rate with the term $m\xi_0^2$ in Ref. [41]. In the case $\delta \neq 0$ the driving is a function of T. Imposing $\frac{d}{dt}T(t) = 0$ one gets from Eq. (12) the MF temperature in the steady state

$$T^{\rm mf} = \left(\frac{H_{\rm dr}}{G_r A}\right)^{2/(3-2\delta)} , \tag{13}$$

the generalization of the Enskog equilibrium solution for a homogeneously driven granular gas [41]. The scaling exponent of $T^{\rm mf}$ in Eq. (13) is $2/3$ for $\delta = 0$, while it is 2 for $\delta = 1$. For $\delta \geq 3/2$ the MF theory does not admit a stable equilibrium state. If $\delta > 3/2$ the driving rate grows faster than the dissipation rate. $\delta = 3/2$ is a limiting case for which the equilibrium state is unstable against density fluctuations. A more detailed stability analysis is far from the scope of this paper, since the typical perturbation around the steady state often also relies on a Maxwellian velocity distribution, which we do not find numerically.

The final approach to the steady state can be obtained by linearizing Eq. (12) around $T^{\rm mf}$, what leads to an exponentially fast approach to equilibrium

$$T^{\rm mf} - T(t+t_0) = T(t_0)\exp\{-[3At_n^{-1} + \delta H_{\rm dr}(T^{\rm mf})^{\delta-1}]t\} , \tag{14}$$

where $t_n^{-1} = G_r\sqrt{T^{\rm mf}}/2$ is the Enskog collision frequency for elastic particles with temperature $T^{\rm mf}$, and $T(t_0)$ is the initial temperature at time t_0. By inserting Eq. (13) in the expression for t_n^{-1}, one can express the characteristic relaxation time $t_{\rm relax} = [\ldots]^{-1}$ as a function of the model parameters, which reduces for $\delta = 1$ to $t_{\rm relax}^{-1} = (5/2)H_{\rm dr}$. Thus, for $\delta = 1$ the characteristic time $t_{\rm relax} = [3At_n^{-1} + \delta H_{\rm dr}(T^{\rm mf})^{\delta-1}]^{-1}$ for the evolution of T towards its equilibrium value does *not* depend on A which contains all the information about the inelasticity. This characteristics is confirmed by numerical simulations (see Fig. 3 below).

3.2 Rough particles with translational driving

Setting to zero the temporal derivatives in Eqs. (7) and (8), one obtains the steady state properties of the driven system with $J_{\rm dr} = 0$ and, for the sake of simplicity, $\delta = 0$:

$$T_{\rm rot}^{\rm mf} = \left(\frac{H_{\rm dr}}{G\Gamma_{\rm tr}}\right)^{2/3} , \quad \text{and} \quad T_{\rm tr}^{\rm mf} = T_{\rm rot}^{\rm mf}/R , \tag{15}$$

with $\Gamma_{\rm tr} = \left(C/B^3\right)^{1/2}\left(CA - B^2\right)$, and $R = B/C$.

Starting from this mean field result for both translational and rotational degrees of freedom, an analysis similar to the one in the previous subsection is possible. Since this did not lead to dramatically new insights, we do not discuss it further. Note, however, that the relaxation times for the translational and rotational degrees of freedom can be strongly different from each other [6].

3.3 Rough particles with rotational driving

Setting to zero the temporal derivatives in Eqs. (7) and (8), one obtains the steady state properties of the rotationally driven system with $H_{\rm dr} = 0$:

$$T_{\rm rot}^{\rm mf} = \left(\frac{J_{\rm dr}}{G\Gamma_{\rm rot}}\right)^{2/3} , \quad \text{and} \quad T_{\rm tr}^{\rm mf} = T_{\rm rot}^{\rm mf}/R \ , \tag{16}$$

with $\Gamma_{\rm rot} = 2\left(B/A^3\right)^{1/2}\left(CA - B^2\right)$, and $R = A/B$. A more detailed analysis of this quasi steady state mean field solution, the approach to the steady state, the parameter dependencies, and the velocity distributions is to be published elsewhere.

4 Numerical simulations

Most of our event driven (ED) molecular dynamics simulations, see [6, 9, 11, 12] for details, with the driving specified above, are first equilibrated without driving and with elastic interactions ($r = 1$, and $r_t = -1$), until the velocity distribution is close to a Maxwellian. Then, dissipation and driving are switched on. However, we checked that the steady state does not depend on the initial conditions. The simulations are performed at a volume fraction $\nu = 0.34$ with $N = 1089$ ($f_{\rm dr} = 133\,{\rm s}^{-1}$) or $N = 11025$ ($f_{\rm dr} = 67\,{\rm s}^{-1}$), and different values of r and r_t. (In our simulations with translational driving, we have chosen $a = 10^{-3}\,{\rm m}$ and $H_{\rm dr} = 1.0\,{\rm s}^{-1}$ so that, for example, $G_r = 8\nu v_r/\sqrt{\pi}ag(\nu) = 3.1 \times 10^3\,{\rm s}^{-1}$, $T^{\rm mf} = 0.0358$ and thus $t_n^{-1} = 2.9 \times 10^2\,{\rm s}^{-1}$, if $r = 0.90$ is used.) With these typical values and a homogeneous driving ($\delta = 0$), the model of a driven granular gas is very close to a homogeneous state; no clusters are observed and the velocity distribution is almost Maxwellian. This is in contradiction to the experimental findings [14, 18], and suggests that the correct representation of the driving in those experiments is *not the homogeneous white noise* usually implemented.

4.1 Approach to steady state

In Figs. 2a-d we compare the solution of the MF equation (13) for a multiplicative driving with $\delta = 1$ to numerical simulations with $N = 11025$, $\nu = 0.34$, and different $r = 0.99$, 0.995, 0.997, 0.998. As one can see, the transient dynamics is quite well reproduced by the MF theory, in the limit of low dissipation (quasi-elastic) considered in the simulations. In the steady state, intermittent behavior is evidenced, however, we do not present a more detailed statistical analysis here.

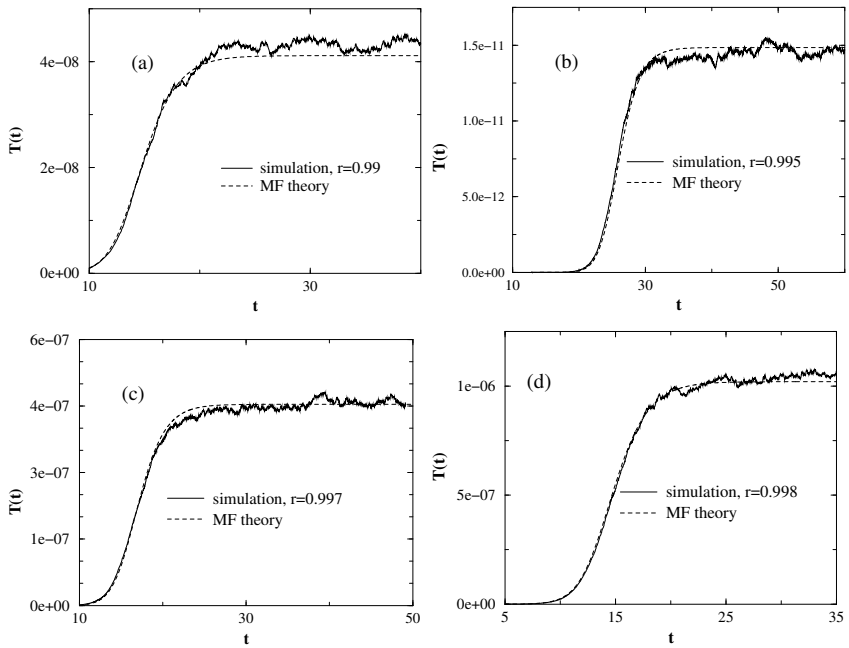

Fig. 2. (a)-(d) Comparison between the solution of the MF equation (13) and numerical simulations for $N = 11025$, $\nu = 0.34$, $\delta = 1$ and $r = 0.99$ (a), $r = 0.995$ (b), $r = 0.997$ (c) $r = 0.998$ (d).

4.2 Relaxation time

In Fig. 3 we check another prediction of the MF theory, i.e. the independence of the characteristic time $t_{\rm relax}$ of the near-to-equilibrium relaxation to the steady state, from the parameter $A = (1 - r^2)/4$ which contains inelasticity. In the figure we compare the normalized MF temperature $T(t)/T^{\rm mf}$ and the normalized numerical temperature $T(t)/T^{\rm eq}$ computed for $r = 0.99$, 0.995, 0.997, 0.998. Because of noise in the initial conditions and dynamics with respect to the MF steady state, the simulation time t has to be translated by an offset time t_0 (with a different value of t_0 for each simulation) in order to collapse the data. The fact that the numerical data collapse onto the MF curve, supports the MF prediction of the independence of the characteristic time from inelasticity in the case $\delta = 1$.

4.3 Steady state temperature

In Fig. 4 we plot the ratio between the numerical results for long times $T^{\rm eq}$ and the theoretical equilibrium temperatures $T^{\rm mf}$ as function of r for different δ. The agreement of the simulations with the MF prediction is optimal for $r \to 1$.

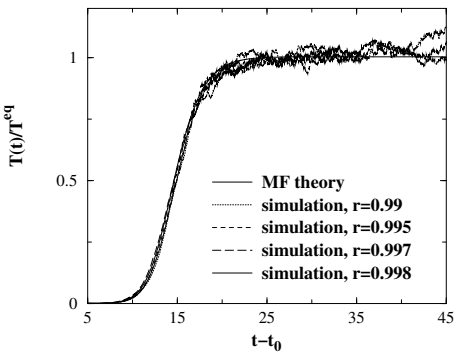

Fig. 3. Comparison between the approach to equilibrium of the normalized MF Temperature $T(t)/T^{\rm mf}$ and the normalized numerical values $T(t)/T^{\rm eq}$ for $N = 11025$, $\nu = 0.34$, $\delta = 1$ and $r = 0.99, 0.995, 0.997, 0.998$. The numerical data collapse onto the MF curve, supporting the MF previsions of the independence of the characteristic time $t_{\rm relax}$ from inelasticity in the case $\delta = 1$.

For $\delta < 0$, the range of agreement extends to much smaller r values, i.e. to stronger dissipation, as in the case of $\delta = 1$ and even in the case $\delta = 0$. One could naively think that the more negative is δ the more favorized should be the homogeneous state. In fact, this is not true. We have performed simulations with $\delta = -1$, and found that the driving is very singular in the low velocity limit, since an excessive amount of energy is given to slow particles.

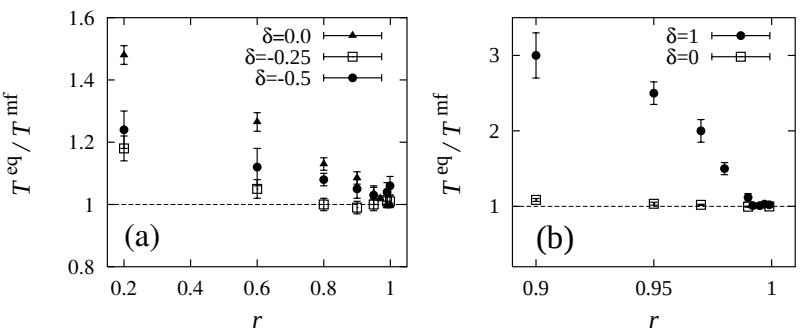

Fig. 4. Rescaled translational temperature $T^{\rm eq}/T^{\rm mf}$ plotted against the restitution coefficient r for $N = 11025$ and different values of δ as given in the insets. Note the different axis scaling in (a) and (b).

4.4 System size dependence

In Fig. 5, the ratio between equilibrium temperature from simulations and MF temperature from the theory, $T^{\rm eq}/T^{\rm mf}$, is plotted against r for two system sizes $N = 11025$ and 5476. The deviation from unity, i.e. the discrepancy between theoretical prediction and numerical simulation of the model, is somewhat larger for the smaller system. For both system sizes, the quality of the theory is perfect in the limit $r \to 1$, within the statistical fluctuations.

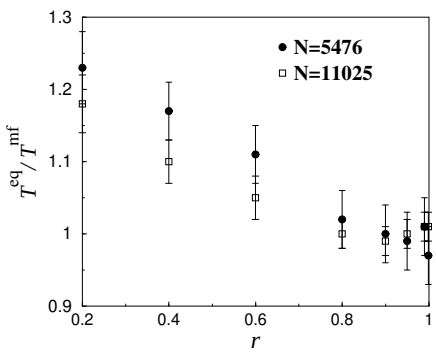

Fig. 5. Rescaled translational temperature $T^{\rm eq}/T^{\rm mf}$ plotted against the restitution coefficient r for two values $N = 11025$, 5476, and $\delta = -0.25$.

4.5 Steady state clustering

In Fig. 1(a-c) snapshots of the system's steady state were shown for $r = 0.999$ (a) $r = 0.97$ (b) and $r = 0.6$ (c), for the more interesting case $\delta = 1$, rather than for the classical $\delta = 0$. Different regimes are observed: A homogeneous state exists for very weak dissipation ($r = 0.999$, Fig. 1(a), whereas dense, persistent clusters with a crystalline structure, domain boundaries, and vacancies are found for higher dissipation ($r = 0.97$). The region between these clusters appears rather homogeneous and dilute (gas-like), very similar to the structures observed in experiments [14, 18]. For higher dissipation ($r = 0.6$) the clusters appear less symmetric, are smaller, and evolve more dynamically.

Note that the clustering in the case $\delta = 1$ is qualitatively different from the case of homogeneous driving, and it appears already for quite high values of r (see Fig. 1). Homogeneous driving, in fact, leads to transient clusters, i.e. they appear and disappear continuously, while in the experiments [14, 18] and in the case of multiplicative driving, the individual clusters are in equilibrium with a gas phase and are stable for rather long times. Simulations with negative δ, (we used $\delta = -0.5$ and $\delta = -0.25$) give a behavior qualitatively similar to

the case of homogeneous driving ($\delta = 0$). For $\delta = 1$, the particles inside the cluster, with rather small relative velocities, are much less agitated than the particles in the surrounding gas phase, so that a cluster is stable. For $\delta \leq 0$, the particles in the cluster are driven comparatively strong, what leads to less stable, dynamic clusters.

5 Simulations with rotation

In Fig. 6 we present the stationary (steady-state) values of $T_{\rm rot}$, normalized by the MF value $T_{\rm rot}^{\rm mf}(r = 0)$, and of the ratios $R = T_{\rm rot}/T_{\rm tr}$, as obtained from numerical simulations and theory for a system of $N = 11025$ particles, with volume fraction $\nu = 0.34$, $r_t = 1$, and r ranging from 0.99 to 10^{-4}. Surprisingly, the agreement with the MF prediction is very good, even *for the lowest value* $r = 10^{-4}$ of the normal restitution, which corresponds to very strong dissipation, where the deviation from MF theory is of the order of only 10%.

To give an example, if the system is driven on the translational degrees of freedom, the stationary temperatures show deviations of $30 - 40\%$ from MF predictions already for $r = 0.6$, see [11] and the previous section. The snapshot in Fig. 1(d) shows the particle distribution for $r = 0.1$ and appears spatially homogeneous – apart from small density fluctuations not quantified here. Thus, rotational velocities are characterized by good homogenization at low r; however, also the translational velocity distribution shows strong deviations from a Maxwellian as will be quantified in the next section. This deviation is due to the rather high dissipation. Numerical simulations with $r = 0.99$ give a Maxwellian distribution for both rotational and translational velocities.

In order to check the role of the tangential restitution, we show in Fig. 7 the stationary values of R with $r = 0.1$ and $r_t \in [-1, 1]$. While for positive r_t there is still good agreement with MF theory, strong deviations appear as $r_t \to -1$. Note that many realistic materials obey the relation $r_t \approx 0.4$ [45], what renders our mean field approach still acceptable.

Our conclusions are that the driving on the rotational degrees of freedom is able to keep the spatial homogeneity of the system up to very high dissipation rates, for positive values of r_t. This leads to a very good agreement of the stationary temperatures with the MF predictions. There are two possible reasons for this. First, the driving acts on rotations. Then, it cannot favorize collisions, since it does not increase the normal component of the relative velocity of the colliding particles. Second, the increase of rotational energy triggered by the driving leads to a shearing force between particles, which reduces density fluctuations and should destroy the translational velocity correlations - but astonishingly does not. When $r_t \to -1$, i.e. in the smooth limit, the agreement with the MF is lost. To explain this result one has to remember that $1 + r_t$ is a measure for the strength of the coupling. Not

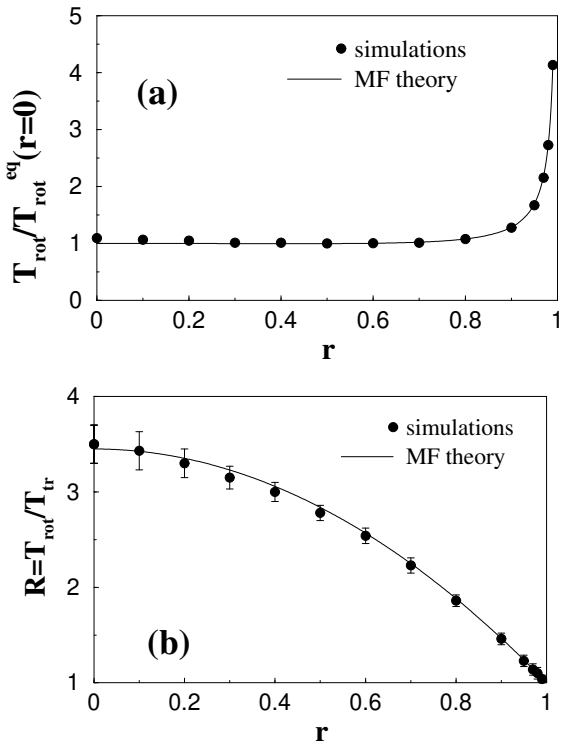

Fig. 6. Simulation (points) and theory (lines) for the parameters $\nu = 0.34$, $N = 11025$, and $r_t = 1$, plotted against r. (a) Stationary rotational temperature $T_{\rm rot}$, normalized by the MF value $T_{\rm rot}^{\rm mf}(r=0)$ at $r=0$. (b) Ratio of stationary rotational and translational temperature $R = T_{\rm rot}/T_{\rm tr}$.

enough rotational energy is transferred to the translational degree, so that the randomization on collisions does not take place. Thus, it is not surprising that MF is no more valid in this very singular limit. Snapshots of the particle distribution for $r = 0.1$ and r_t near to -1 (not displayed here) show indeed stronger density fluctuations in the system as reported in Fig. 1(d).

6 Analytical study of the velocity distribution

In order to study analytically the shape of the velocity distribution function, we extend the approach used by van Noije et al. [32, 33] in the special case $\delta = 0$ to arbitrary δ. The Enskog-Boltzmann equation for the freely cooling gas of spheres, with the standard collision integral $I(f, f)$, has to be extended by the multiplicative driving term proportional to the particle velocity. The

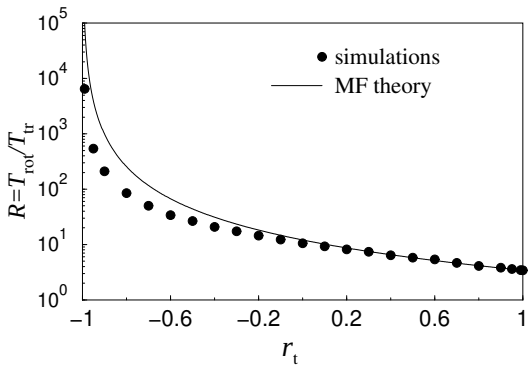

Fig. 7. Simulation (points) and theory (lines) results for $R = T_{\rm rot}/T_{\rm tr}$, with parameters $\nu = 0.34$, $N = 11025$, and $r = 0.1$, plotted against r_t.

Enskog-Boltzmann equation, see Eq. (26) in [32, 33], corrected by a Fokker-Planck diffusion term, is

$$\frac{\partial}{\partial t} f(\vec{v}_1, t) = g(\nu) I(f, f) + \frac{H_{\rm dr}}{2m} \frac{\partial^2}{\partial \vec{v}_1^2} \left[v_1^{2\delta} f(\vec{v}_1, t) \right] \ . \tag{17}$$

Considering the stationary limit $\partial f(\vec{v}_1, t)/\partial t = 0$, and introducing a scaled distribution function, $f(\vec{v}) = (n/v_0^2)\, \tilde{f}(c)$, with the dimensionless velocity $c = v/v_0$ and the mean thermal velocity v_0, one obtains a dimensionless evolution equation for the scaled $f(\vec{v})$, as in [32, 33]. Multiplied by c_1^p and integrated over $\vec{c}_1$, this leads to the following set of equations which couple the moment $\langle c^{p-2+2\delta} \rangle$ to the p-th moment μ_p of the collision term:

$$\frac{H_{\rm dr}}{2 v_0^3 g(\nu) n a} p^2 \left\langle c^{p-2+2\delta} \right\rangle = \mu_p \ . \tag{18}$$

In the special case $\delta = 1$ and $p = 2$, one obtains (for dimensions $d = 2$)

$$\frac{H_{\rm dr}^{1-\delta}}{2 v_0^3 g(\nu) n a} 2 \langle c^2 \rangle = \mu_2. \tag{19}$$

and observing that $\langle c^2 \rangle = v_0^2$ we obtain the stationary value of the thermal velocity in terms of μ_2.

$$v_0 = H_{\rm dr}/(g(\nu) \mu_2 a n). \tag{20}$$

For $\delta \neq 1$ and $\delta \neq 0$ the MF thermal velocity can be obtained by assuming

$$\langle c^{2\delta} \rangle = [\langle c^2 \rangle]^\delta = v_0^{2\delta}. \tag{21}$$

This step is certainly valid for $\delta = 0$ and $\delta = 1$. For real values of δ, we see *a posteriori* that the step leads to the correct MF theory (see previous section),

but we have no clear justification for it. If this assumption, as it seems, turns out to be true, it could probably have interesting implications.

For high c, the rescaled collision term can be approximated by

$$\tilde{I}(\tilde{f},\tilde{f}) \approx -\beta_1 c_1 \tilde{f}(c_1), \tag{22}$$

with $\beta_1 = \pi^{1/2}$ in 2D and the equation for $f(c)$ becomes

$$-\beta_1 c\tilde{f}(c) + \frac{\mu_2}{2d}\left(\frac{\mathrm{d}^2}{\mathrm{d}c^2} + \frac{d-1}{c}\frac{\mathrm{d}}{\mathrm{d}c}\right)[c^{2\delta}\tilde{f}(c)] = 0\ . \tag{23}$$

Inserting a solution of the form $\tilde{f}(c) \propto \exp(-Bc^\alpha)$, we obtain the large c solution $\alpha = \frac{3-2\delta}{2}$ and $B = \frac{2}{3-2\delta}\sqrt{2d\beta_1/\mu_2}$. In particular, for $\delta = 1$ we find $\alpha = 1/2$ what corresponds to the exponent $\alpha = 0.49(3)$ we find in the low r limit (see Fig. 8). Our explanation is that there is a crossover velocity c^* above which the tail with exponent $1/2$ appears, which decreases as r decreases. Such a tail is not observed numerically for high r values, since c^* is outside the velocity range we can examine within reasonable averaging time.

6.1 Translational driving with $\delta = 1$

In the following, we focus on the steady state velocity distribution. Therefore, we performed a large series of simulations for different values of r, with $\nu = 0.34$, $\delta = 1$, and both $N = 1089$ and $N = 11025$. For each value of r we performed about 10^3 simulations for $N = 1089$ and about 200 simulations for $N = 11025$, each with different initial configurations. The distribution of velocity is symmetric and isotropic so that we present only the data for the x component.

For data analysis, a Gaussian with the width obtained from the numerical simulations can be superposed to the velocity distribution function $f(v_x)$ in order to visualize the differences. Furthermore, as a more quantitative approach, a three parameter fit function $f_\alpha(v_x) = f_0 \exp(-B|v_x - \langle v_x\rangle|^\alpha)$ is used to estimate the exponent α of the tail of the distribution. The results are reported in Fig. 8, where a representative velocity distribution is shown in the inset. The main outcome of our simulations is that the velocity distribution is not Gaussian for high inelasticity and that the exponent α in the stretched exponential depends on the normal restitution r. The non-Gaussian behavior is limited to the tail for large r, but seems to extend over the whole range of velocities if r is small enough.

In Fig. 8, the exponent α, for multiplicative driving with $\delta = 1$, varies continuously between 0.49(3) and 1.99(3) and, in particular, for $N = 1089$ and $r = 0.9$ we get $\alpha = 1.05(4)$, while for $N = 11025$ and $r = 0.95$ we observe $\alpha = 1.02(3)$. Such an almost exponential velocity distribution has recently been observed in experiments on a vibrated monolayer of spheres, together with the cluster structure discussed above [14, 18, 19].

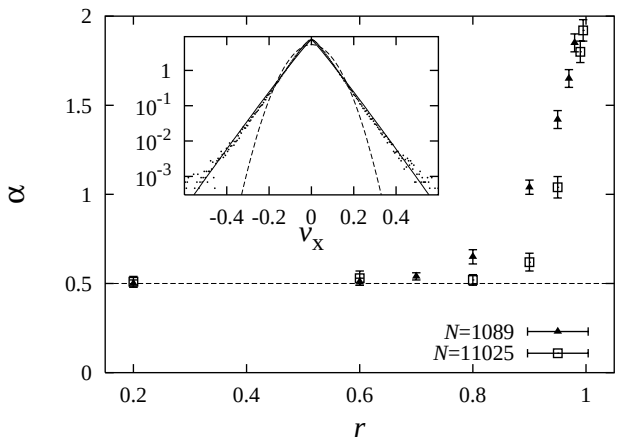

Fig. 8. Plot of the exponent α as a function of r, for $\delta = 1$ and system sizes $N = 1089$ (solid triangles) and $N = 11025$ (open squares). In the inset, the dots give the averaged, normalized velocity distribution from simulations with $N = 1089$ and $r = 0.9$, the solid line is a fit according to $f_\alpha(v_x)$ with $f_0 = 7.6$, $B = 18.9$ and $\alpha = 1.05(9)$, and the dashed line is a Gaussian with the same standard deviation as the data.

6.2 Multiplicative driving with non-integer values of δ

In Fig. 9, for comparison with the results obtained with $\delta = 1$ we show the values of the exponent α, for multiplicative driving with $\delta = 0.5$. The exponent α, in this case, varies continuously between 1.08(3) and 1.99(3) and to get exponents similar to those observed in experiments we have to go down to $r = 0.6$, which is far too small than typical experimental values ($r \sim 0.9$). The value $\delta = 1$ for multiplicative driving, seems then to best fit the experimental findings.

Finally, in Fig. 10 the values of the exponent α, for multiplicative driving with $\delta = -0.25$ and -0.5 are plotted. We see that the velocity distribution is very near to a Gaussian even for strong dissipation, as one would expect from the good agreement of mean field theory and simulations even for small r. For $\delta = -0.5$ the distribution is Gaussian for all value of r.

Simulations with $\delta = -0.5$, -0.25, and 0.5 (see Figs. 9 and 10) and small r ($r = 0.05$ for $\delta = -0.5$, -0.25 and $r = 0.2$ for $\delta = 0.5$) give 1.99(3), 1.77(3), and 1.08(3), quite near to the values 2.0, 7/4, and 1, given by the large c analysis. It interesting to note that for $\delta = -0.5$ the theory predicts $\alpha = 2.0$ for all values of r, i.e. some Gaussian distribution. Our numerical simulations support this result. This does not mean, however, that MF is valid everywere. In fact, we observe both for $\delta = -0.5$ and for $\delta = -0.25$ that the velocity distribution has an anomalously large variance for very low r, so

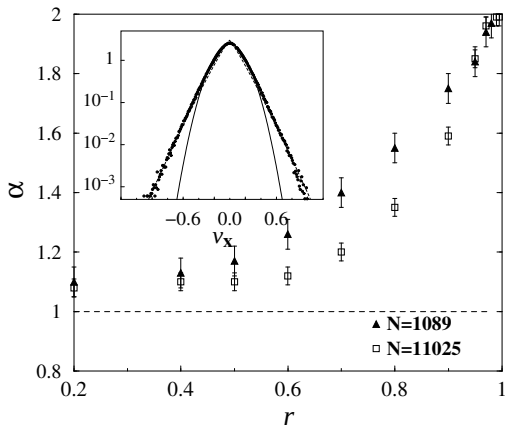

Fig. 9. Plot of the exponent α as a function of r, for $\delta = 0.5$ and system sizes $N = 1089$ (solid triangles) and $N = 11025$ (open squares). In the inset, the dots give the averaged, normalized velocity distribution from simulations with $N = 1089$ and $r = 0.6$, the solid line is a fit according to $f_\alpha(v_x)$ with $f_0 = 3.1$, $B = 1.1$ and $\alpha = 1.12(5)$, and the dashed line is a Gaussian with the same standard deviation as the data.

for $\delta = -0.5$ the distribution is a Gaussian, in the sense that is it quadratic in the velocity, but it is not a Maxwellian, since it has anomalously large fluctuation, which do not correspond to the MF predictions. This explains the small, but not negligible, deviations from MF the one observes for low r in Fig. 4(a). Furthermore, we see from Fig. 4 that a discrepancy between simulations and MF exists even for $\delta = -0.5$. Our explanation is that the driving with $\delta = -0.5$ is such that it preserves the Gaussian shape of the velocity distribution but not its parameters. The velocity fluctuations, i.e. the temperature fluctuations, are anomalously large with respect to the mean.

The behavior at low and intermediate velocity and the effect of spatial inhomogeneities are more difficult to analyze theoretically. In fact, one should solve the Fokker-Planck equation with the full collision integral taking into account the inhomogeneities – maybe an unachievable task. However the following heuristic argument can give an insight in the origin of the non-universal behavior of the velocity distribution at intermediate velocities. Since the driving depends on the velocity, it acts on all the velocity scales, affecting the shape of $f(v)$ in a more complex way than in the case of homogeneous driving. Moreover, when inhomogeneities are present, the driving will depend on the local thermal velocity $v_0(\vec{x})$ *and* on the local density $n(\vec{x})$, while homogeneous driving is *identical everywhere*. Since inhomogeneities are generated by the dissipation, a *feed-back* between driving and dissipation could be at the origin of the non-universal behavior of $f(v)$.

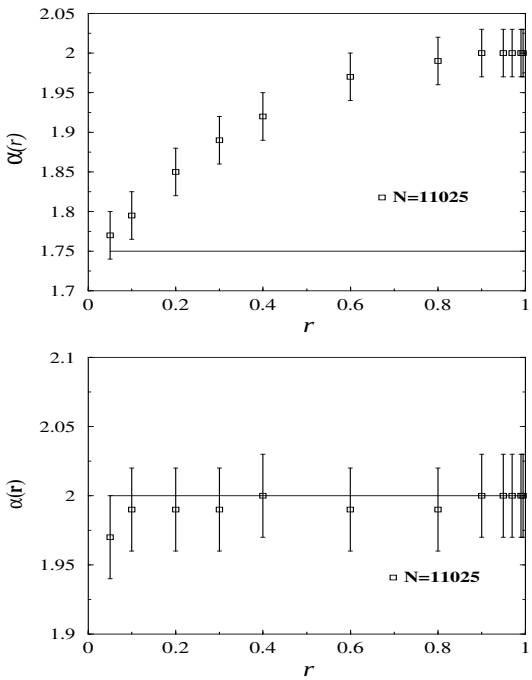

Fig. 10. Plot of the exponent α as a function of r, for system size $N = 11025$, and multiplicative driving with $\delta = -0.25$ (a), and $\delta = -0.5$ (b). The symbols give the simulation results, the error-bars denote the uncertainty in the fit, and the line gives the theoretical prediction.

6.3 Rotations and their distribution

In Fig. 11, we show the stationary rotational and translational velocity distributions for $r = 0.1$, with the other parameters as above. The rotational velocity distribution is very near to a Maxwellian. A three parameter fit $f(x) = A\exp(-B|(x - \langle x\rangle)/\sigma|^{\alpha})$, where $\sigma = \left(\langle (x - \langle x\rangle)^2\rangle\right)^{1/2}$, and x either equals ω or v, is plotted as dashed line in Fig. 11. The parameters $\langle\omega\rangle$, $\langle v\rangle$ and σ are taken from the simulations, and the fit gives $\alpha = 1.92(6)$ for ω, while we obtain $\alpha = 1.41(6)$ for v. This last value is quite near to the value $3/2$ obtained theoretically in Ref. [32]. The applicability of the approach of [11, 32] to the present case, however, has to be discussed since originally a translationally driven, granular gas of smooth particles was considered.

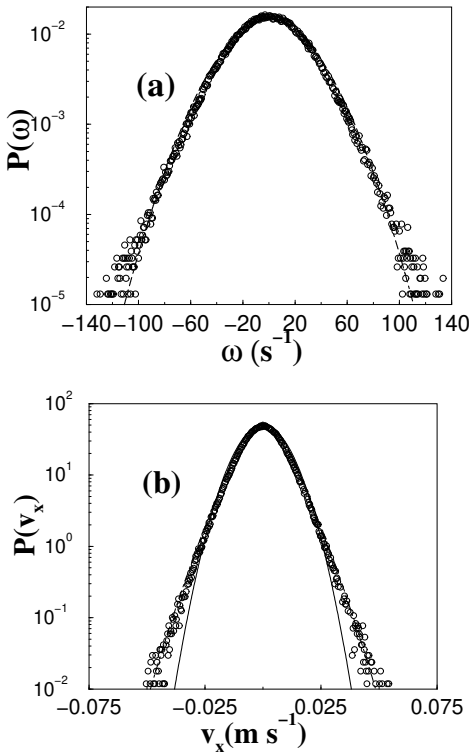

Fig. 11. Steady state rotational (a) and translational (b) velocity distributions for $N = 11025$, $\nu = 0.34$, $r_t = 1.0$ and $r = 0.1$. A power law fit (dashed line) gives an exponent $\alpha = 1.92(6)$ for the rotational distribution and $\alpha = 1.41(6)$ for the translational distribution (see text for details). For comparison, a Maxwellian (solid line) is plotted in (b).

7 Summary and Conclusions

We presented a study of a granular gas subject to both translational driving *proportional* to a power δ of the local velocity and to rotational driving (independent of the angular velocity). Numerical simulations and a theoretical analysis of this model for positive values of δ reproduce qualitatively some experimental findings of [14, 18], which could not be accounted for by homogeneous driving ($\delta = 0$). Furthermore, numerical simulations and theory for negative values of δ and for rotational driving show good homogeneization of the system up to very low values of the restitution coefficient, r, i.e. very strong dissipation.

A microscopic justification for the multiplicative driving is still lacking and requires more detailed experiments or three-dimensional simulation [34] studies. However, as suggested in [11], there is a possible experimental check

of our ideas. From MF theory the scaling of the equilibrium temperature of the vertically vibrated gas with the area fraction ν is given by $T^{\mathrm{mf}} \propto [\nu g(\nu)]^{-2/(3-2\delta)}$. Experimental measurement of the equilibrium temperature of the vertically vibrated monolayer for different values of ν could allow to estimate the value of δ and to verify the hypothesis of a multiplicative effective driving.

Another result of the present study is that both the driving of the rotational degrees of freedom and a multiplicative driving with negative δ are able to keep the spatial homogeneity of the system up to very high dissipation rates – at least for positive values of r_t, i.e. strong coupling between rotational and translational degrees of freedom. This leads to a very good agreement of the stationary temperatures with the MF predictions.

Given the good agreement between MF prediction and simulations, this indicates that deviations from a Maxwellian are not necessarily related to clustering. Moreover, one can have a good agreement of the second moment (the temperature) of the velocity distribution with MF theory together with a non Maxwellian velocity distribution. This poses a theoretical challenge, since some theories for translationally driven granular gases, relate clustering to fat tails in the velocity distribution. The reason why clusters do not occur in our situation, possibly due to the fact that vortices in their early stage are destroyed by the rotational driving, is another issue for future studies.

A possible setup for an experiment with rotational driving is the following: Each extremely rough granular sphere contains a small magnetic bar (to reduce the effect of dipole-dipole interaction at collision). The plane on which the spheres move should be extremely smooth, in order to avoid energy dissipation. Then, spatially homogeneous magnetic pulses periodically spaced in time can be applied in the horizontal directions. This would be the magnetic analogon of the oscillating plane. If the magnetic field is really spatially homogeneous, the magnetic dipoles of the spheres will receive angular momentum from the field, so only rotations are driven, and this angular momentum will be "randomized" by the collisions, if they are frequent enough. To reach a steady-state, it is necessary to give an initial translational velocity to the particles. We are aware that such an experiment is extremely difficult to realize, but a similar setup seems already operational in Dortmund [M. Markus, private communication]. Another reason to look at rotational driving via magnetic forces is the recent interest in electrostatically driven granular media [46] and in magnetic particles with dipolar interactions [A. Kudrolli, private communication, D. Wolf, private communication].

Acknowledgements

R. C. and H. J. H. acknowledge financial support under the European network project FMRXCT980183; S. L. and H. J. H. acknowledge funding from the

Deutsche Forschungsgemeinschaft (DFG). We thank M. A. Muñoz, E. Trizac, and J. S. Urbach for helpful discussions.

References

1. H. M. Jaeger, S. R. Nagel, and R. P. Behringer. Granular solids, liquids, and gases. *Reviews of Modern Physics*, 68(4):1259–1273, 1996.
2. H. J. Herrmann, J.-P. Hovi, and S. Luding, editors. *Physics of dry granular media - NATO ASI Series E 350*, Dordrecht, 1998. Kluwer Academic Publishers.
3. T. Pöschel and S. Luding, editors. *Granular Gases*, Berlin, 2001. Springer. Lecture Notes in Physics 564.
4. K. R. Mecke and D. Stoyan, editors. *Statistical Physics and Spatial Statistics*, Berlin, 2000. Springer.
5. I. Goldhirsch and G. Zanetti. Clustering instability in dissipative gases. *Phys. Rev. Lett.*, 70(11):1619–1622, 1993.
6. S. Luding, M. Huthmann, S. McNamara, and A. Zippelius. Homogeneous cooling of rough dissipative particles: Theory and simulations. *Phys. Rev. E*, 58:3416–3425, 1998.
7. S. Luding. Structures and non-equilibrium dynamics in granular media. *Comptes Rendus Academie des Science*, 3:153–161, 2002.
8. P. K. Haff. Grain flow as a fluid-mechanical phenomenon. *J. Fluid Mech.*, 134:401–430, 1983.
9. M. Huthmann and A. Zippelius. Dynamics of inelastically colliding rough spheres: Relaxation of translational and rotational energy. *Phys. Rev. E*, 56(6):6275–6278, 1998.
10. S. McNamara and W. R. Young. Dynamics of a freely evolving, two-dimensional granular medium. *Phys. Rev. E*, 53(5):5089–5100, 1996.
11. R. Cafiero, S. Luding, and H. J. Herrmann. Two-dimensional granular gas of inelastic spheres with multiplicative driving. *Phys. Rev. Lett.*, 84:6014–6017, 2000.
12. R. Cafiero, S. Luding, and H. J. Herrmann. Rotationally driven gas of inelastic rough spheres. *Europhys. Lett.*, 60(6):854–860, 2002.
13. A. Kudrolli and J. P. Gollub. Studies of cluster formation due to collisions in granular material. In *Powders & Grains 97*, page 535, Rotterdam, 1997. Balkema.
14. J. S. Olafsen and J. S. Urbach. Clustering, order and collapse in a driven granular monolayer. *Phys. Rev. Lett.*, 81:4369, 1998. cond-mat/9807148.
15. W. Losert, D. G. W. Cooper, and J. P. Gollub. Propagating front in an excited granular layer. *Phys. Rev. E*, 59:5855, 1999.
16. W. Losert, D. G. W. Cooper, J. Delour, A. Kudrolli, and J. P. Gollub. Velocity statistics in vibrated granular media. *Chaos*, 9(3):682–690, 1999. cond-mat/9901203.
17. W. Losert, L. Bocquet, T. C. Lubensky, and J. P. Gollub. Particle dynamics in sheared granular matter. *Phys. Rev. Lett.*, 85(7):1428–1431, 2000. cond-mat/0004401.
18. J. S. Olafsen and J. S. Urbach. Velocity distributions and density fluctuations in a 2d granular gas. *Phys. Rev. E*, 60:R2468, 1999.

19. A. Prevost, D. A. Egolf, and J. S. Urbach. Forcing and velocity correlations in a vibrated granular monolayer. *Phys. Rev. Lett.*, 89:084301, 2002.
20. J. T. Jenkins and S. B. Savage. A theory for the rapid flow of identical, smooth, nearly elastic, spherical particles. *J. Fluid Mech.*, 130:187–202, 1983.
21. J. T. Jenkins and M. W. Richman. Kinetic theory for plane shear flows of a dense gas of identical, rough, inelastic, circular disks. *Phys. of Fluids*, 28:3485–3494, 1985.
22. A. Goldshtein and M. Shapiro. Mechanics of collisional motion of granular materials. Part 1. General hydrodynamic equations. *J. Fluid Mech.*, 282:75–114, 1995.
23. S. B. Savage. Analyses of slow high-concentration flows of granular materials. *J. Fluid Mech.*, 377:1–26, 1998.
24. José Maria Montanero and Andrés Santos. Computer simulation of uniformly heated granular fluids. *Granular Matter*, 2(2):53–64, 2000. cond-mat/0002323.
25. I. Goldhirsch and T. P. C. van Noije. Green-Kubo relations for granular fluids. *Phys. Rev. E*, 61:3241–3244, 2000.
26. V. Garzó. Tracer diffusion in granular shear flows. cond-mat/0204268, 2002.
27. A. Barrat and E. Trizac. Lack of energy equipartition in homogeneous heated binary granular mixtures. *Granular Matter*, 4(2):57–63, 2002.
28. I. Pagonabarraga, E. Trizac, T. P. C. van Noije, and M. H. Ernst. Randomly driven granular fluids: Collisional statistics and short scale structure. *Phys. Rev. E*, 65(1):011303, 2002.
29. Y. L. Duparcmeur, H. J. Herrmann, and J. P. Troadec. Spontaneous formation of vortex in a system of self motorised particles. *J. Phys. I France*, 5:1119–1128, 1995.
30. A. Puglisi, V. Loreto, U. M. B. Marconi, and A. Vulpiani. Clustering and non-gaussian behavior in granular matter. *Phys. Rev. Lett.*, 81:3848, 1998.
31. C. Bizon, M. D. Shattuck, and J. B. Swift. Linear stability analysis of a vertically oscillated granular layer. *Phys. Rev. E*, 60:7210–7216, 1999.
32. T. P. C. van Noije and M. H. Ernst. Velocity distributions in homogeneously cooling and heated granular fluids. *Granular Matter*, 1(2):57–64, 1998.
33. T. P. C. van Noije and M. H. Ernst. Velocity distributions in homogeneous granular fluids: the free and the heated case. cond-mat/9803042, 1998.
34. X. Nie, E. Ben-Naim, and S. Y. Chen. Dynamics of vibrated granular monolayers. *Europhys. Lett.*, 51(6):679–648, 2000. cond-mat/9910371.
35. S. McNamara and S. Luding. Energy flows in vibrated granular media. *Phys. Rev. E*, 58:813–822, 1998.
36. A. Puglisi, V. Loreto, U. M. B. Marconi, and A. Vulpiani. A kinetic approach to granular gases. *Phys. Rev. E*, 59:5582–5595, 1999.
37. C. Bizon, M. D. Shattuck, J. B. Swift, and H. L. Swinney. Velocity correlations in driven two-dimensional granular media. In J. Karkheck, editor, *Dynamics: Models and Kinetic Methods for Nonequilibrium Many-Body Systems*, pages 361–371, Dordrecht, 2000. Kluwer Academic Publishers. cond-mat/9904135.
38. T. P. C. van Noije, M. H. Ernst, and R. Brito. Spatial correlations in compressible granular flows. *Phys. Rev. E*, 57:R4891, 1998.
39. T. P. C. van Noije, M. H. Ernst, E. Trizac, and I. Pagonabarraga. Randomly driven granular fluids: Large scale structure. *Phys. Rev. E*, 59:4326–4341, 1999.
40. A. Kudrolli and J. Henry. Non-gaussian velocity distributions in excited granular matter in the absence of clustering. *Phys. Rev. E*, 62(2):R1489–92, 2000. cond-mat/0001233.

41. T. P. C. van Noije, M. H. Ernst, and R. Brito. Ring kinetic theory for an idealized granular gas. *Physica A*, 251:266–283, 1998.
42. S. McNamara and S. Luding. Energy nonequipartition in systems of inelastic, rough spheres. *Phys. Rev. E*, 58:2247–2250, 1998.
43. D. Henderson. A simple equation of state for hard discs. *Mol. Phys.*, 30:971–972, 1975.
44. L. Verlet and D. Levesque. Integral equations for classical fluids. III. the hard disks system. *Mol. Phys.*, 46(5):969–980, 1982.
45. S. F. Foerster, M. Y. Louge, H. Chang, and K. Allia. Measurements of the collision properties of small spheres. *Phys. Fluids*, 6(3):1108–1115, 1994.
46. I. S. Aranson, B Meerson, P. V. Sasorov, and V. M. Vinokur. Phase separation and coarsening in electrostatically driven granular media. *Phys. Rev. Lett.*, 88(20):204301, 2002.
47. see the paper by N. Brilliantov et al. in this book.
48. see the paper by T. Pöschel et al. in this book.
49. see the paper by A. Goldshtein et al. in this book.
50. see the paper by E. ben Naim et al. in this book.
51. see the paper by M. Ernst et al. in this book.